

## Evaluation of the Effect of Viscous Heating in Capillary Rheometry of Polymer Melts

Seppo Syrjälä and Johanna Aho

Tampere University of Technology, Laboratory of Plastics and Elastomer Technology,  
P.O. Box 589, FI-33101 Tampere, Finland

### ABSTRACT

Viscous heating in capillary rheometry of polymer melts is studied by means of numerical simulation. The equations of continuity, momentum and energy are solved along with appropriate viscosity model and boundary conditions using the finite element method. Calculated results for a polycarbonate melt demonstrate a substantial contribution from viscous heating. A significant role played by the pressure dependence of viscosity is also illustrated.

### INTRODUCTION

It is well known that when a highly viscous liquid like polymer melt is deformed in a flow field, some of the work of deformation is converted into heat by internal friction<sup>1,2</sup>. Most polymers have a high viscosity and a low thermal conductivity, which in combination with large process shear rates can lead to a significant increase in temperature.

The effects of viscous heating upon viscosity measurements, particularly in capillary rheometers at high shear rates, is also an important issue<sup>3,4,5</sup>. In the capillary rheometer experiments, the temperature of the fluid being measured is generally assumed to remain at the set temperature throughout the capillary. For polymer melts, however, viscous heating effects are often large enough to cause markedly non-isothermal conditions to occur. As a result,

owing to the temperature-dependent viscosity of polymer melts, the use of the standard equations aimed at determining the viscosity from the isothermal capillary flow can lead to appreciably erroneous viscosity results.

Recently Bur et al.<sup>6</sup> used a non-contact temperature monitoring technique based on fluorescence spectroscopy to measure the temperature of a polymer during capillary rheometry testing. The tests were conducted for polycarbonate and polyethylene melts and a substantial temperature rise was recorded for both materials.

Less well recognized is the fact that the experimental conditions which cause problems with viscous heating often involve pressures sufficiently high for the pressure dependence of viscosity to play a role, too. Sedláček et al.<sup>7</sup>, among others, has experimentally investigated the pressure dependence of viscosity of polymer melts and showed its importance particularly for amorphous polymers.

This paper investigates the combined effects of viscous heating and pressure dependence of viscosity in the capillary flow of polymer melts by means of numerical simulation. The equations of continuity, momentum and energy are solved along with the viscosity model that accounts for the dependence on shear rate, temperature and pressure.

## PROBLEM FORMULATION

Consider the axially symmetric creeping flow of a generalized Newtonian fluid through a capillary. The description of the flow is based on the equations of continuity, momentum and energy, which in the cylindrical coordinate system can be written as follows:

$$\frac{1}{r} \frac{\partial}{\partial r}(ru) + \frac{\partial w}{\partial z} = 0 \quad (1)$$

$$-\frac{\partial p}{\partial z} + \frac{1}{r} \frac{\partial}{\partial r} \left[ \eta r \left( \frac{\partial u}{\partial z} + \frac{\partial w}{\partial r} \right) \right] + \frac{\partial}{\partial z} \left( 2\eta \frac{\partial w}{\partial z} \right) = 0 \quad (2)$$

$$-\frac{\partial p}{\partial r} + \frac{1}{r} \frac{\partial}{\partial r} \left( 2\eta r \frac{\partial u}{\partial r} \right) + \frac{\partial}{\partial z} \left[ \eta \left( \frac{\partial u}{\partial z} + \frac{\partial w}{\partial r} \right) \right] = 0 \quad (3)$$

$$\rho C_p \left( w \frac{\partial T}{\partial z} + u \frac{\partial T}{\partial r} \right) = k \left[ \frac{1}{r} \frac{\partial}{\partial r} \left( r \frac{\partial T}{\partial r} \right) + \frac{\partial^2 T}{\partial z^2} \right] + \eta \dot{\gamma}^2 \quad (4)$$

In the above equations,  $z$  and  $r$ , respectively, denote the axial and radial coordinates,  $w$  and  $u$ , respectively, are the axial and radial velocity components,  $p$  stands for the pressure,  $T$  is the temperature and  $\eta$ ,  $\rho$ ,  $C_p$  and  $k$ , respectively, designate the viscosity, density, specific heat and thermal conductivity of the polymer. The term  $\eta \dot{\gamma}^2$  in the energy equation represents viscous heating. Under the present flow field, the shear rate,  $\dot{\gamma}$ , takes the form

$$\dot{\gamma} = \left[ 2 \left( \frac{\partial u}{\partial r} \right)^2 + 2 \left( \frac{u}{r} \right)^2 + 2 \left( \frac{\partial w}{\partial z} \right)^2 + \left( \frac{\partial u}{\partial z} + \frac{\partial w}{\partial r} \right)^2 \right]^{1/2} \quad (5)$$

The material property values used in the simulations are those corresponding to polycarbonate (PC) Calibre 200-10 (Dow) used in the experiments of Bur et al<sup>6</sup>. The viscosity function is described as

$$\eta = \alpha \eta_o [1 + (\alpha \lambda \dot{\gamma})]^{n-1} \quad (6)$$

The shift factor,  $\alpha$ , is taken to contain the contribution from temperature and pressure, that is

$$\alpha = \alpha_T \alpha_p \quad (7)$$

The temperature shift factor is determined from the WLF equation of the form

$$\log(\alpha_T) = \frac{8.86(T_o - T_s)}{101.6 + (T_o - T_s)} - \frac{8.86(T - T_s)}{101.6 + (T - T_s)} \quad (8)$$

The pressure shift factor is calculated from the exponential relation given by

$$\alpha_p = \exp(\beta p) \quad (9)$$

The adjusting parameters in the above equations were specified as follows:  $\eta_o = 2858$  Pa s,  $\lambda = 0.007$  1/s,  $n = 0.336$ ,  $T_o = 270^\circ\text{C}$ ,  $T_s = 165^\circ\text{C}$  and  $\beta = 30 \cdot 10^{-9}$  1/Pa. Most of these values were taken from the Campus data bank<sup>8</sup> (corresponding to PC Calibre 200-10), but the last parameter  $\beta$  was estimated on the basis of the experiments of Sedláček et al.<sup>7</sup>. For the density, specific heat and thermal conductivity the following values were

used:  $\rho = 1100 \text{ kg/m}^3$ ,  $C_p = 2100 \text{ J/(kg}^\circ\text{C)}$  and  $k = 0.25 \text{ W/(m}^\circ\text{C)}$ . The capillary used in the experiments of Bur et al.<sup>6</sup> had the length of 30 mm and the diameter of 1 mm and these values were adopted for the present study.

The velocity boundary conditions consist of imposing the no-slip condition at the capillary wall, the fully developed condition at the capillary inlet (corresponding to the inlet melt temperature) and the zero derivative condition at the capillary outlet. The thermal boundary conditions are the uniform melt temperature at the inlet ( $270^\circ\text{C}$ ) and the zero derivative condition at the outlet. At the capillary wall, both the isothermal ( $270^\circ\text{C}$ ) and adiabatic conditions are considered. It is obvious that the true thermal boundary condition at the capillary wall is intermediate between these two extremes. In the figure captions below, these boundary conditions are referred to as BC1, meaning the adiabatic capillary wall, and BC2, meaning the isothermal capillary wall. Numerical solutions to the above equations were obtained by the finite element method using the Comsol Multiphysics computer program<sup>9</sup>.

## RESULTS AND DISCUSSION

Calculations were carried out for the apparent shear rates ranging from 50 1/s to 2000 1/s. The predicted maximum and mean melt temperatures at the capillary outlet as a function of apparent shear rate are displayed in Fig. 1 indicating a significant temperature rise for both boundary conditions. Interestingly, the melt temperatures measured by Bur et al.<sup>6</sup> most closely correspond to the predicted maximum temperatures with the adiabatic capillary wall condition. The predicted temperature developments along the capillary are illustrated in Fig. 2. As expected, for the adiabatic thermal boundary condition the maximum temperature occurs on the

capillary wall, and for the isothermal condition somewhere inside the capillary.

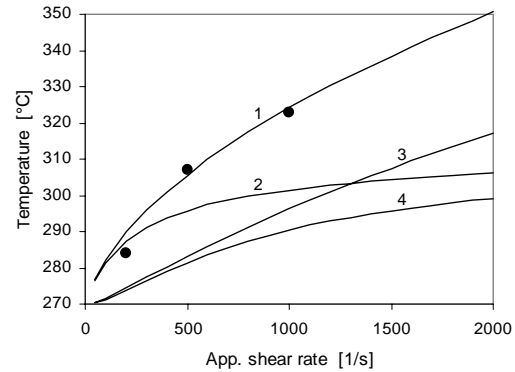


Figure 1. Predicted maximum temperatures ( $T_{max}$ ) and mean temperatures ( $T_m$ ) of the melt at the outlet of the capillary as a function of apparent shear rate: (1)  $T_{max}$  for BC1, (2)  $T_m$  for BC1, (3)  $T_{max}$  for BC2, (4)  $T_m$  for BC2 (• measured<sup>6</sup>).

The predictions for the pressure drop across the capillary as a function of apparent shear rate are shown in Fig. 3 for both capillary wall boundary conditions. Additionally, the results of the simulation neglecting the temperature and pressure dependence of viscosity are given. In these simulations, the material property values were taken at the inlet melt temperature ( $270^\circ\text{C}$ ). Hence, these predictions should correspond to the usual assumptions behind the capillary rheometer measurements. It can be seen that for the adiabatic capillary wall condition the results are below and for the isothermal capillary wall condition above the ones obtained by ignoring the temperature and pressure dependence of viscosity. That is, the contribution of the viscous heating appears to be more significant in the case of the adiabatic wall boundary condition, whereas the contribution of the pressure dependence of viscosity is larger in the case of the isothermal wall boundary condition. In principle, these two contributing factors may compensate for each other in some circumstances.

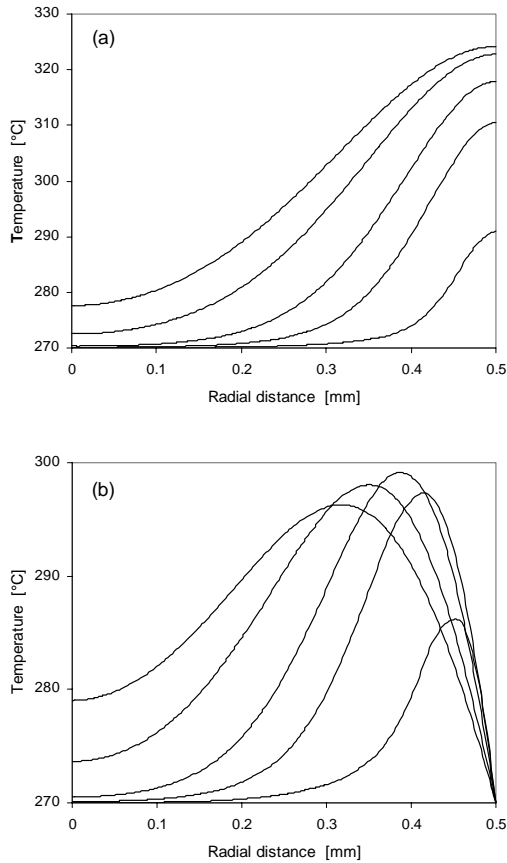


Figure 2. Predicted development of temperature along the capillary for the apparent shear rate of 1000 1/s; (a) BC1, (b) BC2 (results are shown at axial distances of 1, 5, 10, 20 and 30 mm)

The predictions for the axial distribution of pressure with the apparent shear rate of 1000 1/s are depicted in Fig. 4. The simulation with the temperature and pressure independent viscosity results in a linear pressure profile, which in accordance with the basic theory of capillary rheometry. The other two pressure profiles show significant deviations from the linear behaviour. This is expected since both the viscous heating and the pressure dependence of viscosity tend to contribute to the curvature of the pressure profile.

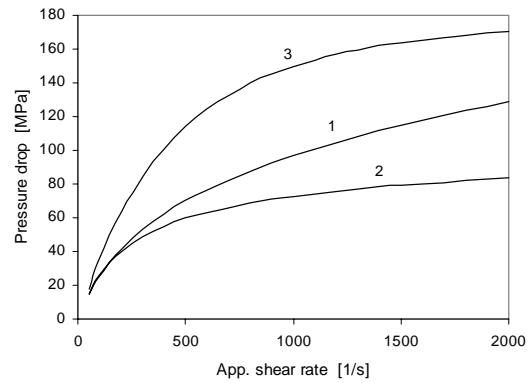


Figure 3. Predicted pressure drop across the capillary as a function of apparent shear rate; (1) temperature and pressure independent viscosity, (2) BC1, (3) BC2.

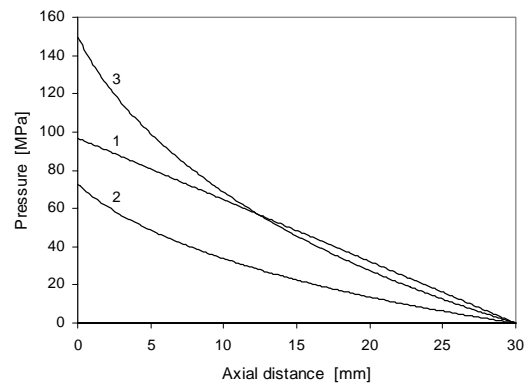


Figure 4. Predicted axial distributions of pressure for the apparent shear rate of 1000 1/s; (1) temperature and pressure independent viscosity, (2) BC1, (3) BC2.

## CONCLUSIONS

Significant effects of the viscous heating and pressure dependence of viscosity in the capillary rheometry of polymer melts were demonstrated by employing numerical simulation. It is, however, worth pointing out that the viscosity of polycarbonate is highly sensitive to temperature and pressure compared to most other polymers.

## REFERENCES

1. Cox, H.W. and Macosko, C.W. (1974), "Viscous Dissipation in Die Flows", *AICHE J.*, **20**, 785-795.
2. Winter, H.H. (1977), "Viscous Dissipation in Shear Flows of Molten Polymers", *Adv. Heat Transfer*, **13**, 205-267.
3. Hieber, C.A. (1977), "Thermal Effects in the Capillary Rheometry", *Rheol. Acta*, **16**, 553-567.
4. Rosenbaum, E.E. and Hatzikiriakos, S.G. (1996), "The Effect of Viscous Heating in Capillary Rheometry", *SPE ANTEC Tech. Papers*, **42**, 1080-1084.
5. Szabo, P. (2002), "Evaluation of Measurements from Capillary Rheometers Influenced by Viscous Heating", *Transaction of the Nordic Rheology Conference*, **10**, 127-130.
6. Bur, A.J., Roth, S.C. and Lobo, H. (2002), "Temperature Effects during Capillary Rheometry Testing", *SPE ANTEC Tech. Papers*, **48**, 3405-3409.
7. Sedláček, T., Zatloukal, M., Filip, P., Boldizar, A. and Sába, P. (2004), "On the effect of pressure on the shear and elongational viscosities of polymer melts", *Polym. Eng. Sci.*, **44**, 1328-1337.
8. [www.campusplastics.com](http://www.campusplastics.com)
9. Comsol Multiphysics, Version 3.3, User's Guide.